

# Long-Term Composition Dynamics of PAH-Containing NAPLs and Implications for Risk Assessment

CATHERINE A. PETERS,\*  
CHRISTOPHER D. KNIGHTS, AND  
DERICK G. BROWN

*Department of Civil and Environmental Engineering,  
Princeton University, Princeton, New Jersey 08544*

Subsurface contaminants such as coal tar, creosote, diesel fuel, and other petroleum-derived materials typically exist as very complex chemical mixtures. Risk assessment is useful for site management if a single metric can represent the composition-dependent risk profile of the mixture. This paper examines the factors governing human health risk assessment for multicomponent nonaqueous phase liquids (NAPLs) containing polycyclic aromatic hydrocarbons (PAHs). A model is presented describing the interdependence of the dissolution rates of individual compounds and the shifts in the NAPL composition that occur due to the large differences in aqueous solubilities. The model also accounts for solidification of the less soluble NAPL constituents. Thirty-year numerical simulations describe composition dynamics for natural environmental processes as well as three remediation processes: pump-and-treat, bioremediation, and solvent extraction. Carcinogenic risk due to ingestion of contaminated groundwater at the source is estimated, and its dependence on contaminant removal and NAPL composition shifts is described. When composition dynamics are slow, a compound like naphthalene has great potential to contribute to risk because it may persist in groundwater. When there is significant depletion of the lower molecular weight compounds, the risk is dominated by contributions from compounds such as benzo[a]pyrene. Remediation technologies have the greatest potential for risk reduction if they are effective in removing the more carcinogenic, high molecular weight compounds. Because PAHs can contribute to risk for different reasons and because of the interdependence of their behaviors, compositional approaches lead to better risk predictions for PAHs than simple lumped metrics such as total petroleum hydrocarbon (TPH).

## Introduction

Polycyclic aromatic hydrocarbons (PAHs) represent an important class of environmental pollutants because several PAHs are suspected carcinogens, and cancer has been associated with long-term exposure to mixtures of PAHs (1). Of the 1430 hazardous waste sites on the National Priority List (NPL), PAHs have been found at over 600 of these (2). One of the most important forms of environmental pollution involving PAHs is subsurface contamination from nonaqueous phase liquid (NAPL) contaminants such as coal tar,

creosote, diesel fuel, and other petroleum-derived materials. Coal tars, which are almost entirely composed of PAHs, exist as subsurface contaminants at former manufactured gas plant (MGP) sites because of the historical disposal of industrial byproducts (3).

The total cost to the nation estimated for cleaning up hazardous waste sites over the next 30 yr is \$750 billion (4). The enormity and complexity of this problem necessitates application of appropriate criteria for site prioritization and setting of cleanup goals. Hazardous waste site management is complicated by the fact that PAH contaminants typically exist as very complex mixtures, of which no single compound predominates. For PAHs, tracking individual compounds can be an onerous task since many PAH-containing NAPLs contain very large numbers of compounds. On the other hand, lumping PAHs together may not be acceptable because of the large range of physical, chemical, and toxicological properties of these compounds. Contaminated soils and sediments containing hydrocarbon wastes are often characterized by measurements of total petroleum hydrocarbons (TPH). Such a lumped metric obscures the valuable information that chemical composition can provide. A risk assessment approach for decision-making regarding hazardous waste sites can be particularly beneficial for complex mixture contaminants. With appropriate integration procedures, the contaminant can be characterized using a single metric that represents the composition-dependent risk profile of the mixture.

This paper presents a modeling analysis of the release of PAHs from multicomponent NAPLs and an examination of the factors governing human health risk assessment for these contaminants. A mathematical model of long-term NAPL composition dynamics is presented. Because PAHs represent a range of aqueous solubilities, there is considerable potential for shifts in the NAPL composition as it is exposed to ambient groundwater. Selective dissolution can result in solidification of the less soluble constituents. Also, the behaviors of the individual PAH compounds are strongly interdependent deriving from the phase equilibrium thermodynamics governing NAPL dissolution. These effects are demonstrated through illustrative simulations of hypothetical NAPLs that are representative of coal tar contaminants. The predicted concentrations in groundwater are integrated with a risk assessment calculation to estimate carcinogenic risk associated with ingestion of the contaminated water. The effects of natural as well as engineered remediation processes, including pump-and-treat, solvent extraction, and bioremediation, are explored.

## Risk Determinants for PAHs

The human health risk posed by a chemical is determined by its inherent toxicity and by the receptor population's potential for exposure (5). Exposure to subsurface contaminants may occur via several possible exposure pathways (6), but in this paper we consider the carcinogenic risk posed by ingestion of contaminated groundwater in direct contact with PAH-containing NAPLs. PAHs are particularly interesting because the higher molecular weight compounds are more carcinogenic, but the lower molecular weight compounds are more soluble in the groundwater and thus have a greater potential to reach receptors.

**Toxicity.** This paper focuses on carcinogenic risk, which has traditionally been the risk assessment basis for benzene and PAHs. Noncarcinogenic toxicological effects are potentially important, but risk assessment protocols have yet to be standardized for these effects. We refer the reader to the

\* Corresponding author telephone: (609)258-5645; fax: (609)258-2799; e-mail: cap@princeton.edu.

TABLE 1. Toxicity Classifications of PAHs and Reported Toxic Equivalency Factors

	EPA priority pollutants	EPA Group B2 carcinogens	NTP carcinogens	IARC Group 2 carcinogens	EPA TEF (10)	Nisbet/LaGoy TEF (11)
naphthalene	X					0.001
2-methylnaphthalene	X					0.001
acenaphthylene	X					0.001
acenaphthene	X					0.001
fluorene	X					0.001
phenanthrene	X					0.001
anthracene	X					0.01
fluoranthene	X					0.001
pyrene	X					0.001
benz[a]anthracene	X	X	X	X	0.1	0.1
chrysene	X	X			0.001	0.01
5-methylchrysene			X	X		
benzo[a]pyrene	X	X	X	X	1	1
benzo[b]fluoranthene	X	X	X	X	0.1	0.1
benzo[j]fluoranthene			X	X		
benzo[k]fluoranthene	X	X	X	X	0.01	0.1
7H-dibenzo[c,g]carbazole			X	X		
benzo[g,h,i]perylene	X					0.01
indeno[1,2,3-c,d]pyrene	X	X	X	X	0.1	0.1
dibenz[a,h]anthracene	X	X	X	X	1	5
dibenz[a,h]acridine			X	X		
dibenz[a,i]acridine			X	X		
dibenzo[a,e]pyrene			X	X		
dibenzo[a,h]pyrene			X	X		
dibenzo[a,i]pyrene			X	X		
dibenzo[a,j]pyrene			X	X		

work of the TPH Criteria Working Group, which has compiled health effects data for a broad range of hydrocarbon contaminants and has proposed a risk-assessment framework that accounts for both carcinogenic and noncarcinogenic risk (7).

Under the weight-of-evidence classification scheme, the U.S. Environmental Protection Agency (EPA) has identified seven PAHs as probable human carcinogens on the basis of sufficient evidence in animal studies (Group B2) (Table 1). The EPA lists the other PAHs as not classifiable (Group D); however, there have been recent discussions suggesting that naphthalene may be more appropriately classified as a possible human carcinogen (Group C) (8). The National Toxicology Program (NTP) has identified 15 PAHs as "reasonably anticipated to be human carcinogens" (9). These PAHs include six of the seven Group B2 PAHs plus nine additional high molecular weight PAHs (Table 1). The International Agency for Research on Cancer (IARC) has listed the same 15 PAHs in their Group 2 classification, which includes probable and possible human carcinogens (1). On the basis of both animal and human health effects data, the IARC lists coal tars in the most potent classification, Group 1, known human carcinogens.

Benzo[a]pyrene is the only PAH for which toxicological data have been sufficient for derivation of a carcinogenic potency factor. Data are available, however, to quantify the toxicities of other PAHs *relative* to benzo[a]pyrene, expressed as toxic equivalency factors (TEFs). These are used to estimate benzo[a]pyrene-equivalent doses (BaP<sub>eq</sub>dose). For a PAH compound *i*

$$\text{BaP}_{\text{eq}}\text{dose}_i = \text{TEF}_i \times \text{dose}_i \quad (1)$$

The EPA's Office of Health and Environmental Assessment has presented a list of TEFs for the Group B2 PAHs (10) (Table 1). Nisbet and LaGoy (11) also published TEF values for PAHs based on previously published studies (Table 1). An important feature of the latter is the assignment of nonzero TEF values for all EPA priority pollutant PAHs under the reasoning that some, albeit limited, carcinogenic activity has been associated with these compounds. In the present work, the TEF values

of Nisbet and LaGoy are used, which implies that all the priority pollutant PAHs have the potential to contribute to risk. In a companion paper, we examine the different risk outcomes when either the Nisbet and LaGoy or the EPA Group B2 TEFs are used (12).


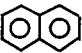
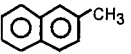
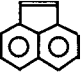
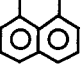

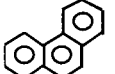
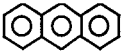
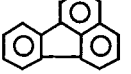

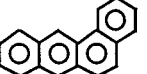
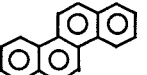
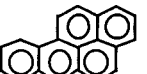
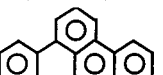
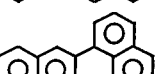
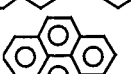
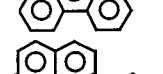
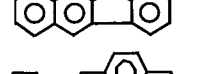
**Potential for Groundwater Contamination.** Listed in Table 2 are the aqueous solubilities for the 17 priority pollutant PAHs as well as for benzene. These values are based on data compiled by Mackay et al. (13) except the aqueous solubility of indeno[1,2,3-*cd*]pyrene, which was obtained from Verscheuren (14). Because NAPL dissolution occurs from a liquid phase and many PAHs are solids in their pure states at ambient temperatures, the true indicator of solubility is the subcooled liquid solubility,  $S_i$ :

$$S_i = \frac{C_{s,i}}{(f^S/f^L)_i} \quad (2)$$

where  $C_{s,i}$  is the aqueous solubility of pure *i* (mg/L) and  $(f^S/f^L)_i$  is the ratio of solid-liquid reference fugacities of pure *i*. The values of  $(f^S/f^L)_i$  listed in Table 2 were computed using data for enthalpy of fusion, melting temperature, and difference in solid/liquid heat capacities where available (15) using the methods described previously (16–18). Otherwise, an approximation was obtained by assuming that the entropy of fusion at the melting temperature is 13.5 cal mol<sup>-1</sup> K<sup>-1</sup>. The solid-liquid reference fugacity ratio decreases with increasing molecular size, as does  $C_{s,i}$ . Consequently, the range of values spanned by  $S_i$  is somewhat less broad than the range for  $C_{s,i}$ , but it still represents order-of-magnitude differences in the dissolution tendencies of PAHs.

The disparity between solubilities of the constituents in a PAH-containing NAPL has significant implications for the behavior of these materials and their potential to contribute to risk. First, the more soluble PAHs generally are less toxic than the higher molecular weight PAHs. Naphthalene is 3 orders of magnitude more soluble than benzo[a]pyrene, but it is at least 3 orders of magnitude less toxic (Table 1). Thus, the low molecular weight PAHs have the potential to contribute to risk because of the potential for high doses.

TABLE 2. EPA Priority Pollutant PAHs plus Benzene and Their Properties<sup>c</sup>

		Mol. Wt. <i>W</i>	Aq. Sol. at 25°C <i>C<sub>s</sub></i> [mg/L]	Biodeg. rate <i>k<sub>B</sub></i> [day <sup>-1</sup> ]	Fug. Ratio at 25°C ( <i>f<sup>S</sup>/f<sup>L</sup></i> )	Initial <i>x<sub>i</sub><sup>N</sup></i>	CERCLA 1997 Ranking
Benzene (BEN)		78	1780	0.1	1	0.03	5
Naphthalene (NPH)		128	31	0.337	0.30	0.17	72
2-Methylnaphthalene (2MN)		142	25	N.A. (a)	0.86	0.08	156
Acenaphthylene (ACY)		152	3.9	0.02	0.22 (b)	0.04	--
Acenaphthene (ACE)		154	3.8	0.01	0.20	0.03	155
Fluorene (FLR)		166	1.9	0.015	0.16	0.05	260
Phenanthrene (PHN)		178	1.1	0.0447	0.28	0.05	232
Anthracene (ANTH)		178	0.05	0.0052	0.010	0.0085	265
Fluoranthene (FLN)		202	0.26	0.0018	0.21	0.02	96
Pyrene (PYR)		202	0.13	0.0027	0.11	0.03	236
Benz[a]anthracene (BaA)		228	0.011	0.0026	0.04 (b)	0.005	38
Chrysene (CHR)		228	0.002	0.0019	0.0097	0.007	116
Benzo[a]pyrene (BaP)		252	0.004	0.0022	0.03 (b)	0.006	8
Benzo[b]fluoranthene (BbFN)		252	0.0015	0.0024	0.039 (b)	0.003	9
Benzo[k]fluoranthene (BkFN)		252	0.0008	0.0005	0.013 (b)	0.003	59
Benzo[g,h,i]perylene (BgHiP)		276	0.0003	0.001	0.003 (b)	0.001	--
Indeno[1,2,3-c,d]pyrene (IPY)		276	0.062	0.0024	0.0451 (b)	0.004	177
Dibenz[a,h]anthracene (DBaHA)		278	0.0005	0.0019	0.004 (b)	0.0006	17

<sup>a</sup> N.A. denotes not available. <sup>b</sup> Enthalpy of fusion data unavailable. <sup>c</sup> See text for data sources. The initial NAPL composition for model simulations is also shown.

The high molecular weight PAHs have the potential to contribute to risk even when present at low concentrations due to their high toxic potencies. The second important implication of the disparity of aqueous solubilities of PAHs is the significant potential for shifts in NAPL composition. As the lower molecular weight compounds dissolve, the NAPL becomes enriched in the high molecular weight PAHs. Because solubility depends on the abundance of the compound in the NAPL phase, the aqueous phase concentrations of the more toxic compounds can increase with time. This implies a complex interdependence of the behavior of NAPL constituents that can only be described with a model that adequately characterizes the composition of the mixture.

Another important risk determinant is persistence in the environment. Compounds that are less soluble also tend to be more recalcitrant to biodegradation. For the PAHs listed in Table 2, first-order biodegradation rate constants are shown. In an effort to be consistent across the compounds, these parameters were selected from a single study for Kidman sandy loam (19), except for benzene (13). There is a strong correlation between solubility and biodegradation rate, implying that the extent to which the lower molecular weight PAHs contribute to risk may be reduced if these compounds are degraded in a timely fashion.

### PAH–NAPL Composition Simulations

Consider a subsurface environment contaminated with a NAPL that is a mixture of PAHs. The mathematical model is designed to describe the temporal profiles of the concentrations in the NAPL phase and in groundwater that contacts the NAPL. The processes of NAPL dissolution and solidification in the field are not completely understood, so we make use of models based largely on mechanistic inferences derived from laboratory studies. In the absence of appropriate field data on the time scale of decades, model predictions cannot be verified, and yet predictions of long-term dynamics are needed for risk assessment. A number of papers have appeared in the literature presenting model simulations and some experimental data of composition dynamics in multi-component NAPLs (20–27). With the exception of Corapcioglu and Baehr (20), the NAPLs that have been considered are relatively simple mixtures of no more than five constituents, primarily composed of compounds that are liquids in their pure states. The model presented here is unique in that it describes a complex mixture, primarily composed of compounds that are solids in their pure states. An important feature of the model is that it allows for the formation of a solid phase, which is pertinent for PAH-containing NAPLs. This extends the capabilities of an earlier version of the model (28) and includes an improved numerical procedure that facilitates simulation of a large number of compounds.

**Model System and Equations.** The model system is the NAPL-contaminated zone of the subsurface and consists of an inert porous medium, a flowing aqueous phase, NAPL held at residual saturation in the porous medium, and possibly solid PAH phases. Each of the two fluid phases is described as being spatially uniform in composition. In this paper, we focus on temporal aspects of compositional shifts. Spatial considerations of NAPL composition variation, solidification, and solute fate and transport beyond the NAPL-contaminated zone are described elsewhere (29).

The processes for the aqueous phase are (i) input of dissolved compounds from the NAPL phase, (ii) flushing from the aqueous phase, and (iii) first-order biodegradation (for the bioremediation scenario). The mass balance for constituent  $i$  in the aqueous phase is

$$\frac{dC_i^A}{dt} = k_{ai}(C_i^* - C_i^A) - \frac{C_i^A}{\tau} - k_{bi}C_i^A \quad (3)$$

where  $C_i^A$  is the concentration of  $i$  in the aqueous phase (mg/L),  $k_{ai}$  is the mass transfer rate constant ( $t^{-1}$ ),  $C_i^*$  is the aqueous phase solubility (mg/L),  $\tau$  is the aqueous phase residence time (t), and  $k_{bi}$  is the biodegradation rate constant ( $t^{-1}$ ). Equation 3 is written in volume-normalized fashion, assuming that the aqueous phase volume does not change significantly. Mass transfer is described using a constant that lumps the mass transfer coefficient (L/t) and the inverse of the characteristic diffusion length (1/L). The solubility is related to NAPL composition through (30–34)

$$C_i^* = x_i^N S_i \quad (4)$$

where  $x_i^N$  is the mole fraction of  $i$  in the NAPL phase. Implicit in eq 4 are several assumptions, most important of which is that the constituent behaves ideally in the NAPL phase with respect to a reference state of pure liquid  $i$  (i.e., Raoult's law assumption). The validity of this assumption for PAH-containing NAPLs has been examined both theoretically (35) and experimentally (17). Equation 4 reveals the importance of NAPL phase composition in governing the interaction in the behaviors of the constituents despite the absence of interactions at the molecular level. The NAPL phase mole fraction may decrease due to dissolution of  $i$  or may increase due to selective extraction of other constituents, which thus changes the driving force for dissolution.

The processes for the NAPL phase are (i) dissolution to the aqueous phase and (ii) precipitation to or dissolution from a solid PAH phase, if it exists. The mass balance for constituent  $i$  in the NAPL phase is

$$W_i \frac{dm_i^N}{dt} = -k_{ai} V^A (C_i^* - C_i^A) - P_i \quad (5)$$

where  $W_i$  is the molecular weight of  $i$  (g/mol),  $m_i^N$  is the moles of  $i$  in the NAPL phase (mol),  $V^A$  is the volume of the aqueous phase ( $L^3$ ), and  $P_i$  is the rate of precipitation (or redissolution) of  $i$ . This mass balance cannot be normalized by the total moles in the NAPL phase,  $\sum m_i^N$ , because this quantity does not remain constant. The mass balance for the solid PAH phase is

$$W_i \frac{dm_i^S}{dt} = P_i \quad (6)$$

where  $m_i^S$  is the moles of solid  $i$  (mol). In the absence of any mechanistic information on the kinetic limitations to NAPL solidification and redissolution, the NAPL and solid PAH phases are considered to be in equilibrium. This assumption is premised on the close proximity of the two phases. However, research is needed to examine this assumption and the potential impact of nonequilibrium on long-term NAPL solidification. With this assumption, solid PAH begins to form when (and if) the constituent's mole fraction in the NAPL phase reaches its solubility limit,  $x_i^{N*}$ . For the case of ideal behavior in the NAPL and solid phases, this solubility limit is equal to the solid–liquid reference fugacity ratio, which is a constant at a given temperature (16, 18):

$$x_i^{N*} = \left( \frac{f^S}{f^L} \right)_i \quad (7)$$

When a solid is present, the value of  $x_i^N$  is constant and is equal to  $x_i^{N*}$ .

**Numerical Solution Procedure.** Equations 3, 5, and 6 provide a set of  $3*n$  coupled differential equations in  $3n$  variables,  $C_i^A$ ,  $m_i^N$ , and  $m_i^S$  for  $i = 1-n$ , where  $n$  is the number of NAPL constituents. A numerical solution procedure has been developed that decouples the aqueous phase equations



from the NAPL and solid-PAH phase equations. The previous time step values for  $C_i^A$  and  $\Sigma m_i^N$  are used as initial guesses for the values at the new time step, and eq 5 is solved analytically for the values of  $m_i^N$ . These values are used along with the new value of  $\Sigma m_i^N$  to compute the new values for  $\bar{C}_i^A$  using eq 3. This process is repeated until convergence. Within the same time step, another iteration loop checks whether any of the constituents have reached their solubility limits in the NAPL phase or whether solid-PAH already exists for any of the constituents. For these compounds, the value of  $P_i$  is computed and  $x_i^N$  is set equal to  $x_i^{N^*}$ . After calculation of all  $P_i$  values,  $m_i^S$ ,  $m_i^N$ , and  $x_i^N$  are updated, and iteration continues until convergence to NAPL/solid-phase equilibrium. Unless otherwise stated, simulations were run for 30-yr time periods, which is consistent with the time frame of the exposure duration parameter in the risk calculation described below.

**Model Parameters and Initial Conditions.** The NAPLs simulated in this work were designed to be representative of coal tars. The compounds for which quantitative toxicity data exist are modeled explicitly, and an uncharacterized fraction is designed to be representative of the remaining NAPL constituents. The initial mole fractions (Table 2) were based on coal tar compositions reported in the literature (30, 36). The uncharacterized fraction, with a mole fraction of 0.46, is modeled as having negligible aqueous solubility and biodegradation rate. The molecular weight of this fraction is taken to be 300 (35). The NAPL density,  $\rho^N$ , is assumed to be 1 g/mL (30). The system temperature is 25 °C.

The total system size is a cubic 125 m<sup>3</sup> volume, and the porosity is 0.4, which is typical of unconsolidated deposits. The base case low-saturation scenario has a NAPL saturation of 0.01, corresponding to an approximate soil TPH level of 2500 ppm. A high-saturation scenario was simulated with a NAPL saturation of 0.1 or 25 000 ppm of soil TPH. These are in the range of saturation values found in the field (37). The aqueous phase residence time was computed assuming a Darcy velocity of 0.4 m/day, which along with the porosity corresponds to the characteristics of the sandy aquifer in Cape Cod, MA (38). The assumed values for porosity, NAPL saturation, and Darcy velocity were used with the parameters: mean grain diameter of 0.05 cm (Cape Cod aquifer), average molecular diffusion coefficient of  $5 \times 10^{-6}$  cm<sup>2</sup>/s, and water kinematic viscosity of 0.0089 cm<sup>2</sup>/s to estimate  $k_a$  of 6.1 day<sup>-1</sup> for the low-saturation scenario and 53 day<sup>-1</sup> for the high-saturation scenario, using the empirical correlation for NAPL dissolution kinetics of Imhoff et al. (39). A common value of  $k_a$  was used for all NAPL constituents because of the small range of molecular diffusivities and because of observations of similar rates of interphase mass transfer for PAHs dissolving from a multicomponent NAPL (17). The values of  $k_a$  and  $\tau$  are assumed to be constant. With the exception of the bioremediation simulation, it is assumed that losses due to biodegradation are negligible.

**Risk Calculation.** The predicted aqueous phase concentrations are used for estimation of carcinogenic risk due to ingestion of the contaminated water. This represents a worst-case scenario with respect to the groundwater exposure pathway in that attenuation processes related to transport and transformation that occur off-site are not considered. Risk is defined as "the upper bound lifetime probability of an individual developing cancer as a result of exposure to a particular level of a potential carcinogen" (40). The total risk due to exposure to the mixture is

$$\text{risk} = \text{SF}_{\text{BaP}} \sum \text{BaP}_{\text{eq}} \text{dose}_i \quad (8)$$

where  $\text{SF}_{\text{BaP}}$  is the oral carcinogenic slope factor for benzo[a]pyrene, and the benzo[a]pyrene-equivalent doses are

determined from the actual doses and the TEF values (eq 1). The summation of benzo[a]pyrene-equivalent doses to give a total effective dose of benzo[a]pyrene is premised on the assumption of concentration additivity, which is appropriate if the chemicals have a similar mode of toxic action (41). While only sparse data exist to validate this assumption for PAHs, general low-level exposures to multiple toxicants such as drinking water contaminants may be considered additive (42). The actual dose for compound  $i$ ,  $\text{dose}_i$ , is the lifetime average daily absorbed dose [(mg of toxicant) (kg of body weight)<sup>-1</sup> day<sup>-1</sup>] and is a product of the time-averaged concentration in water and the factors that determine the average ingestion rate:

$$\text{dose}_i = \bar{C}_i^A \left( \frac{\text{Ir} \times \text{Ef} \times t_{\text{ed}}}{\text{Bw} \times \text{At}} \right) \quad (9)$$

Exposure assumptions were made to be consistent with EPA guidance on default assumptions for the "reasonable maximum exposure" (40, 43) (more currently referred to as the "high-end individual exposure"). The exposure parameters are ingestion rate (Ir) of 2.0 L/day, exposure frequency (Ef) of 350 day/yr, exposure duration ( $t_{\text{ed}}$ ) of 30 yr, and body weight (Bw) of 70 kg. The averaging time (At) is a 70-yr normalizing factor for lifetime cancer risks. The time-averaged contaminant concentrations were calculated by a numerical approximation of the integral:

$$\bar{C}_i^A = \frac{1}{t_{\text{ed}}} \int_0^{t_{\text{ed}}} C_i^A(t) dt \quad (10)$$

The value of  $\text{SF}_{\text{BaP}}$  is 7.3 per (mg/kg) day<sup>-1</sup> (8). Benzene's contribution to risk was computed using its oral carcinogenic slope factor of  $2.9 \times 10^{-2}$  per (mg/kg) day<sup>-1</sup> (8).

## Remediation Scenarios

**Pump-and-Treat.** Pump-and-treat technology has been the most widely applied remediation approach at Superfund sites, with 98% of NPL sites adopting this approach either in exclusion or in combination with other technologies (44). To simulate pump-and-treat remediation of our hypothetical contaminated site, we envision an injection/recovery well scheme that effects an accelerated water flow velocity. The maximum pumping rate is constrained by hydrologic properties and aquifer thickness. We take the effective aquifer thickness to be the vertical depth of the contaminated zone, 5 m, and the distance between the injection and recovery wells to be 10 m. Assuming a hydraulic conductivity of 95 m/day, which is the average value for the sandy aquifer in Cape Cod, MA (45), the maximum Darcy velocity is 48 m/day. Assuming roughly one-tenth of this value for the present simulation (4 m/day), the mass transfer coefficient is 34.1 day<sup>-1</sup>. The pump-and-treat scenario was run for a simulation period of 10 yr, which is a typical time frame for this remediation approach. The resulting NAPL compositions and saturations were then taken to be initial conditions for 30-yr simulations under hydrodynamic conditions corresponding to the original low-saturation or high-saturation scenarios. The risk results were computed by integrating the concentrations for this latter period only.

**Solvent Extraction.** To speed the process of contaminant removal, pumping-based remediation technologies may be augmented through injection of solvents that enhance the solubility of NAPL constituents (46, 47). To simulate solvent extraction of our hypothetical contaminated site, we consider a solvent-water solution of 40% *n*-butylamine, which has been shown to be an effective solvent for enhancing the solubility of coal tar (30). The aqueous phase solubility limit

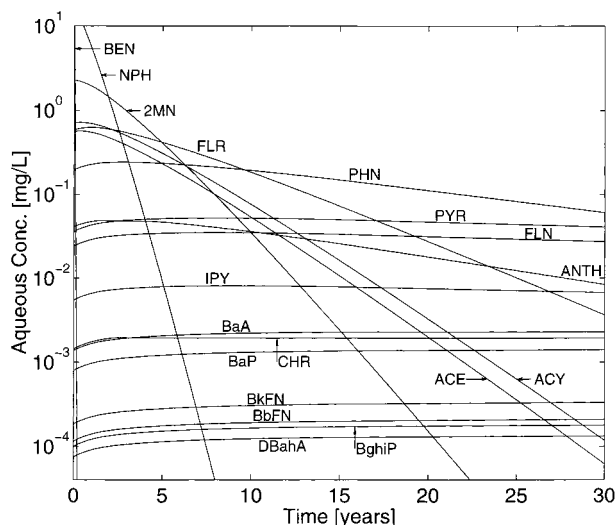


FIGURE 1. Simulated aqueous concentrations versus time for the low-saturation scenario.

(eq 4) is modified as

$$C_i^* = x_i^N \frac{\rho^N}{K_{NS,i}} \frac{W_i}{W_N} \quad (11)$$

where  $W_N$  is the average molecular weight of the NAPL and  $K_{NS,i}$  is the NAPL/solvent partition coefficient for  $i$ . Measured values of  $K_{NS,i}$  for naphthalene, phenanthrene, and pyrene (30) were correlated with  $K_{OW}$  values, resulting in the following linear free energy relationship (LFER):

$$\log K_{NS,i} = 0.61 + 0.14K_{OW,i} \quad (12)$$

This was used to estimate the NAPL/solvent partition coefficients for the other compounds. It is assumed that the solvent does not partition into the NAPL phase and change its properties. The solvent extraction remediation scenario was run for the low-saturation scenario for a simulation period of 1 month. This time period was chosen because the amount of total NAPL removed is comparable to that achieved in 10 yr of pump-and-treat. The resulting NAPL composition and saturation served as the initial conditions for a subsequent 30-yr simulation from which a risk estimate was computed.

**Bioremediation.** Bioremediation applications range from natural attenuation processes to highly engineered technologies involving augmentation of the subsurface with nutrients, microorganisms, and supplemental substrate. The rates of biodegradation achieved under these conditions will be vastly different. The objective in this paper is to describe one plausible bioremediation scenario and focus on the potential for enhanced shifts in NAPL composition due to the differences in biodegradabilities of the PAH constituents. We presume that biodegradation is occurring in the aqueous phase according to the rate constants presented in Table 2. All other model parameters are identical to the low-saturation scenario. This simulation was run for a period of 30 yr, and the risk was determined for this period.

## Simulation Results

**Composition Dynamics.** For the low-saturation scenario, the resulting aqueous phase concentrations and NAPL phase mole fractions are shown in Figures 1 and 2, using the compound abbreviations in Table 2. The concentrations of the lower molecular weight compounds, benzene and naphthalene, are depleted rapidly. The concentrations of slightly less soluble compounds such as 2-methylnaphtha-

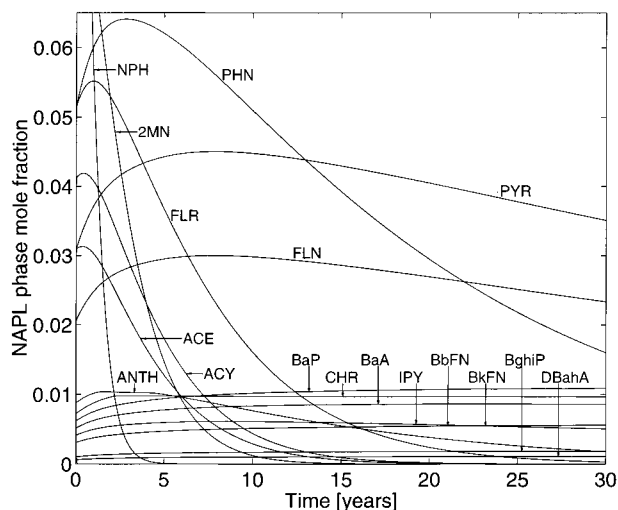


FIGURE 2. Simulated NAPL phase mole fractions versus time for the low-saturation scenario. Benzene is not shown because its mole fraction approaches zero too quickly to be shown on this plot.

lene, acenaphthene, acenaphthylene, and fluorene also decrease significantly over the 30-yr period. The dissolution of these compounds from the NAPL phase causes the mole fractions of the less soluble compounds to increase because their rates of dissolution are relatively slower. The mole fractions of phenanthrene, fluoranthene, and pyrene increase for several years, resulting in an increased driving force for their dissolution and increased aqueous phase concentrations. Eventually, these compounds become the most soluble NAPL constituents, and their concentrations begin to decrease. The concentrations of the higher molecular weight compounds, benzo[a]pyrene, benzo[b]fluoranthene, benzo[k]fluoranthene, benzo[g,h,i]perylene, and dibenz[a,h]anthracene, only increase during the time period of the simulation. For example, benzo[a]pyrene's aqueous concentration increases from its initial value of  $8 \times 10^{-4}$  mg/L to a final value of  $1.4 \times 10^{-3}$  mg/L.

Another important facet of the composition dynamics is the solidification of NAPL constituents. After 1.2 yr, anthracene reaches its mole fraction solubility limit and begins to precipitate. At 2.7 yr, the mass of solidified anthracene reaches a maximum value of 87 g. It has completely redissolved after 4.4 yr at which time the mole fraction of anthracene in the NAPL phase begins to decrease (see Figure 2). Chrysene's mole fraction reaches its limit after 2.1 yr. After 28 yr, the solid chrysene has reached a maximum of 760 g and begins to redissolve. Because only two compounds were found to solidify, the solidification phenomenon is not particularly complex for this simulation. In a paper by Knights and Peters (48), a simulation for a fully characterized coal tar is presented in which solidification and redissolution occur for a large number of constituents.

**Risk Assessment for Low-Saturation Scenario.** The time-averaged aqueous concentrations for the low-saturation simulation result in a total risk of  $4.6 \times 10^{-4}$  (Figure 3a). The greatest contributor is benzo[a]pyrene (28%). Indeno[1,2,3-c,d]pyrene (16%) and dibenz[a,h]anthracene (13%) also contribute significantly to the total risk. The contribution by dibenz[a,h]anthracene is appreciable despite the fact that it is initially the least abundant NAPL constituent. The next largest contributor is naphthalene (10%), which is much less carcinogenic than the top three contributors but has high aqueous concentrations in the early time periods of the simulation. Together, the Group B2 carcinogens account for only 63% of the risk and include the least significant contributors: chrysene (0.4%), benzo[b]fluoranthene (0.4%), and benzo[g,h,i]perylene (0.04%).

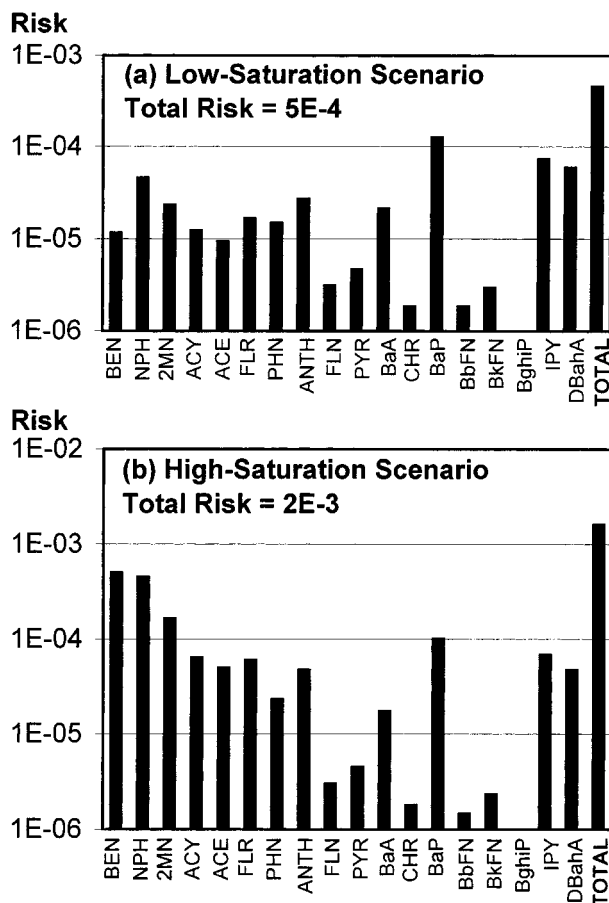


FIGURE 3. Total risk and contributions to risk by individual PAH compounds for the (a) low-saturation and (b) high-saturation scenario simulations.

One can compare the change in total risk with the change in TPH to examine the potential difference in site management using a risk-based approach. A 30-yr risk projection based on the initial NAPL composition is estimated to be  $2.3 \times 10^{-2}$  and is mostly comprised of contributions from benzene and naphthalene. After 5 yr, the composition corresponds to a total risk of  $4.9 \times 10^{-4}$ , a 98% reduction. After 30 yr, the total risk is  $3.2 \times 10^{-4}$ , a 99% reduction. The amount of NAPL in terms of a soil TPH metric changes from its initial value of 2500 ppm to 1950 ppm after 5 yr and then to 1750 after 30 yr, an overall reduction of 30%. Out of the 17 states that have soil TPH cleanup standards, 10 have cutoff values of 100 ppm (49). The modest TPH reduction in the present simulation would not be sufficient to meet this. However, the risk has decreased by 2 orders of magnitude, which may be considered appreciable in a risk-based regulatory approach. It should also be recognized that the total amount of NAPL (and the TPH) continuously decreases while the mole fractions of some of the more toxic compounds increase. Most of the risk reduction has occurred within the first five years, and additional risk reduction over the following decades is extremely slow. The leveling off of the risk reflects the dominance of the risk by compounds whose concentrations are rather constant and even increasing with time. These considerations point to the inadequacy of a TPH metric as an indicator of human health risk reduction.

**Risk Assessment for High-Saturation Scenario.** In comparison to the low-saturation scenario, the high-saturation scenario corresponds to a slightly higher rate of mass transfer to the aqueous phase, but the larger source results in much slower composition dynamics. The lower molecular weight compounds take longer to be depleted and the increase in

the mole fractions of the remaining constituents occurs much slower. The onset of solidification of NAPL constituents is also delayed, with anthracene beginning to solidify after 12 yr and chrysene after 20 yr. The total risk is estimated to be  $1.6 \times 10^{-3}$  (Figure 3b). Despite the fact that the initial NAPL composition is the same as for the low-saturation scenario, the total risk is significantly larger reflecting the slower composition dynamics. The greatest contributors to risk are benzene (31%) and naphthalene (28%), and benzo[a]pyrene is the fourth largest contributor to risk (6.2%).

**Sensitivity Analysis.** A sensitivity analysis was performed for the low-saturation scenario with respect to the parameters governing groundwater flow and interphase mass transfer kinetics. The Darcy velocity was varied from its nominal value by factors of 1/2 and 2. The corresponding range for the value of  $k_a$  is 4.1–11 day<sup>-1</sup>. The low values of Darcy velocity and  $k_a$  result in a total risk of  $5.8 \times 10^{-4}$ , and the high values result in a total risk of  $3.8 \times 10^{-4}$ . Because the correlation used to estimate the mass transfer rate constant is applicable to NAPL held at residual saturation in a uniformly distributed porous medium, we expect that mass transfer rates in the field may be significantly smaller due to NAPL pooling, hydrodynamic fingering, NAPL solidification, etc. To further examine uncertainty in the mass transfer rate constant beyond the range predicted by the correlation of Imhoff et al., we ran a matrix of simulations with  $k_a$  ranging from 0.01 to 10 day<sup>-1</sup> with the same variation in Darcy velocity described above. The risk due to benzene is higher when  $k_a$  is smaller, but the risk due to benzo[a]pyrene is smaller when  $k_a$  is smaller. This inverse behavior of the risk contributions produces a net effect that the total risk is fairly robust, with risk estimates ranging from  $5.3 \times 10^{-5}$  at the high velocity and  $k_a = 0.01$  day<sup>-1</sup> to  $5.8 \times 10^{-4}$  at the low velocity and  $k_a = 4.1$  day<sup>-1</sup>.

**Remediation Simulations.** The pump-and-treat scenario (Figure 4a) results in a slightly smaller risk ( $2 \times 10^{-4}$ ) than the low-saturation scenario, due to enhanced depletion of the lower molecular weight compounds. After 10 yr of pump-and-treat, the concentrations of the larger PAHs, such as benzo[a]pyrene and dibenz[a,h]anthracene, are essentially the same as in the low-saturation scenario. Because most of the risk in the low-saturation scenario is attributable to these compounds, the effectiveness of pump-and-treat is minimal. These results are consistent with field observations of the limited effectiveness of pump-and-treat for removal of NAPL contaminants as has been discussed by Mackay and Cherry (50) and the NRC (4). The pump-and-treat simulation for the high-saturation scenario (not shown) resulted in a larger reduction in risk to a value of  $4 \times 10^{-4}$ , as compared to  $2 \times 10^{-3}$ . In this scenario, the lower molecular weight compounds are the largest contributors to risk, so pump-and-treat is somewhat effective in risk reduction.

Solvent extraction has a much greater potential for risk reduction (Figure 4b). The total risk is predicted to decrease by several orders of magnitude. When a cosolvent is present, the solubilities of all the NAPL constituents increase, but the increase is larger for the higher molecular weight compounds (30). As shown in eq 12, the slope in the LFER is significantly less than unity implying that the range of values for  $K_{NS}$  is much smaller than the range of values for  $K_{OW}$ . Thus, solvent extraction causes a reduction in the bulk NAPL volume without a significant shift in composition that occurs when there are disparities in constituent solubilities.

The risk results for the bioremediation scenario (Figure 4c) are very similar to the low-saturation scenario with respect to both total risk and the distribution of risk. A slight risk reduction resulted, due to small reductions in the concentrations of the lower molecular weight compounds. Presumably, efforts to speed up this process through provision of optimum conditions for biological growth would only



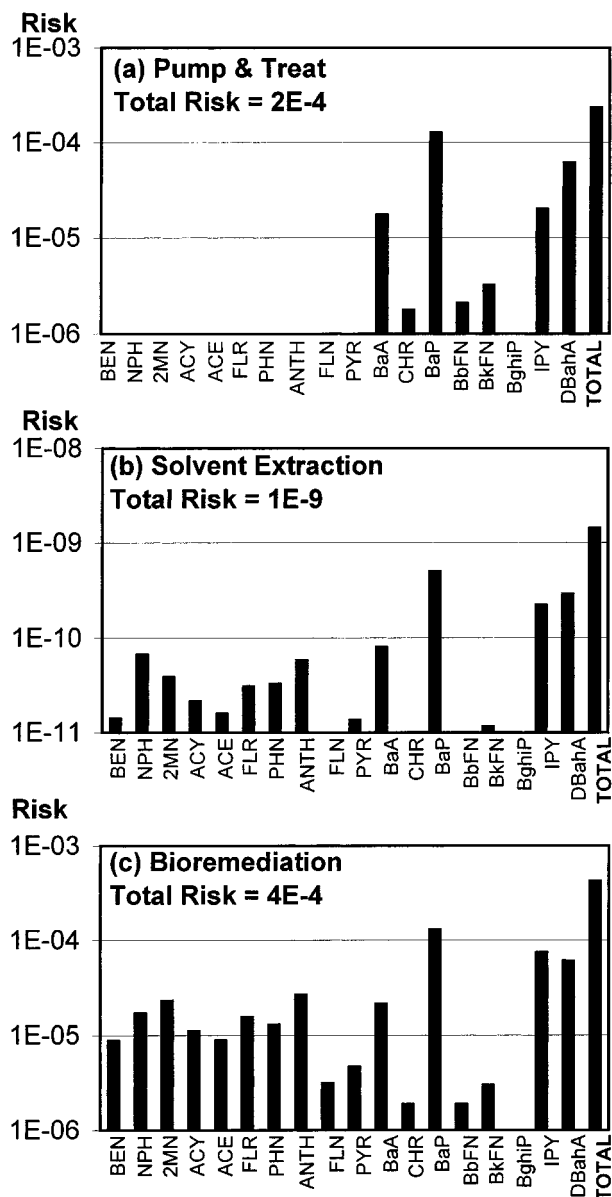


FIGURE 4. Total risk and contributions to risk by individual PAH compounds for the simulated remediation scenarios: (a) pump-and-treat, (b) solvent extraction, and (c) bioremediation.

increase the biodegradation rates of the lower molecular weight compounds, which are more bioavailable and biodegradable. These shifts in NAPL composition may have little effect in terms of order-of-magnitude reduction in risk. Remediation is most effective in risk reduction if it does not selectively operate on the low molecular weight compounds.

## Discussion

The PAH-containing NAPL contaminant and the scenarios examined are hypothetical but not unrealistic. We have demonstrated that significantly different risk outcomes result when the same NAPL is exposed to different environmental conditions or when the NAPL is present at different initial saturations. Compounds that may be important in one scenario may not be significant in another because PAHs contribute to risk for different reasons. Here, we compare the PAH risk ranking results with the CERCLA priority list for hazardous substances (51). Because this list is used to set national priorities for waste management, it is pertinent to see how the prioritization of PAHs compares with the rankings obtained in the present study. The CERCLA rankings for the

compounds included in the present study are shown in Table 2. Benzene and benzo[a]pyrene are the highest ranking, and dibenz[a,h]anthracene is the fourth highest. This is consistent with the present findings, although it is unlikely that all three of these compounds would simultaneously be significant contributors to risk. There are some inconsistencies. For example, CERCLA's lowest ranking PAH is anthracene, but this was found to rank in the top five in a number of the simulations.

This comparison points to the fact that there are no simple guidelines to identify a priori which compounds are of greatest significance. Several different risk rankings resulted even for the limited range of conditions examined in this analysis, demonstrating how sensitive the results are to those site-specific conditions that govern NAPL composition dynamics. However, some generalizations can be made. There is some rationale for focusing on benzo[a]pyrene and dibenz[a,h]anthracene because of their high toxicity and persistence. Similarly there is some rationale for focusing on benzene and naphthalene because of their high concentrations and potential for migration in groundwater. Furthermore, some compounds such as chrysene and benzo[b]-fluoranthene may receive undo attention simply due to classification as Group B carcinogens while their potential to contribute to overall risk may be very small.

We have demonstrated the strong dependence of risk on NAPL composition and the importance of compositional modeling for accurate risk determinations. Because this task may become unmanageable for complex mixtures, risk assessments may best be performed using a fraction approach. Such an approach for PAH-containing NAPLs is discussed in a companion paper (12), which presents an extension of the fraction approach developed by the Total Petroleum Hydrocarbon Criteria Working Group (TPHCWG).

## Acknowledgments

This research was supported by the U.S. Environmental Protection Agency through the Northeast HSRC by Grant Project R-69 and by the U.S. Army Environmental Quality Basic Research Program Work Unit BT25-EC-B08 entitled "Prediction of NAPL Interfacial Properties". The authors also acknowledge the anonymous reviewers whose comments substantially improved the rigor of this presentation.

## Literature Cited

- (1) *Overall Evaluation of Carcinogenicity: An Updating of IARC Monographs Volumes 1 to 42*; IARC Monographs on the Evaluation of Carcinogenic Risks to Humans; International Agency for Research on Cancer: Lyon, France, 1987; Supplement 7.
- (2) *Toxicological Profile for Polycyclic Aromatic Hydrocarbons*; Agency for Toxic Substances and Disease Registry (ATSDR): Atlanta, 1995.
- (3) Luthy, R. G.; Dzombak, D. A.; Peters, C. A.; Roy, S. B.; Ramaswami, A.; Nakles, D. V.; Nott, B. R. *Environ. Sci. Technol.* **1994**, *28*, 266A-276A.
- (4) National Research Council. *Alternatives for Ground Water Cleanup*; National Academy Press: Washington, DC, 1994.
- (5) Loehr, R. C.; Webster, M. T. Effect of Treatment on Contaminant Availability, Mobility, and Toxicity. In *Environmentally Acceptable Endpoints in Soil: Risk-Based Approach to Contaminated Site Management Based on Availability of Chemicals in Soil*; Linz, D. G., Nakles, D. V., Eds.; American Academy of Environmental Engineers: Annapolis, MD, 1997; Chapter 2.
- (6) Labieniec, P. A.; Dzombak, D. A.; Siegrist, R. L. *J. Environ. Eng.* **1996**, *122*, 388-398.
- (7) *Development of Fraction Specific Reference Doses (RfDs) and Reference Concentrations (RfCs) for Total Petroleum Hydrocarbons (TPH)*. Total Petroleum Hydrocarbon Criteria Working Group Series, Vol. 4; Amherst Scientific Publishers: Amherst, MA, 1997.
- (8) *Integrated Risk Information System (IRIS)*; U.S. Environmental Protection Agency, National Center for Environmental Assessment: Cincinnati, OH, 1997.



- (9) *The 8th Report on Carcinogens: 1998 Summary*; National Toxicology Program, National Institute of Environmental Health Sciences: Research Triangle Park, NC, 1998.
- (10) *Provisional Guidance for Quantitative Risk Assessment of Polycyclic Aromatic Hydrocarbons*; Office of Research and Development, U.S. EPA: Washington, DC, 1993; EPA/600/R-93/089.
- (11) Nisbet, I. C. T.; LaGoy, P. K. *Regul. Toxicol. Pharmacol.* **1992**, *16*, 290–300.
- (12) Brown, D. G.; Knightes, C. D.; Peters, C. A. *Environ. Sci. Technol.* **1999**, *33*, 4357–4363.
- (13) Mackay, D.; Shiu, W. Y.; Ma, K. C. *Illustrated Handbook of Physical-Chemical Properties and Environmental Fate for Organic Chemicals*; Lewis Publishers: Chelsea, MI, 1992.
- (14) Verscheuren, K. *Handbook of Environmental Data on Organic Chemicals*, 3rd ed.; Van Nostrand Reinhold: New York, 1996.
- (15) Daubert, T. E.; Danner, R. P. *Physical and Thermodynamic Properties of Pure Chemicals: Data Compilation*; Hemisphere Publishing Co.: New York, 1989.
- (16) Peters, C. A.; Mukherji, S.; Knightes, C. D.; Weber, W. J., Jr. *Environ. Sci. Technol.* **1997**, *31*, 2540–2546.
- (17) Mukherji, S.; Peters, C. A.; Weber, W. J., Jr. *Environ. Sci. Technol.* **1997**, *31*, 416–423.
- (18) Peters, C. A.; Wamner, K. H.; Knightes, C. D. Multicomponent NAPL Solidification Thermodynamics. *J. Transp. Porous Media* In press.
- (19) Park, K. S.; Sims, R. C.; Dupont, R. R. *J. Environ. Eng.* **1990**, *116*, 632–640.
- (20) Corapcioglu, M. Y.; Baehr, A. L. *Water Resour. Res.* **1987**, *23*, 191–200.
- (21) Kaluarachchi, J. J.; Parker, J. C. *J. Contam. Hydrol.* **1990**, *5*, 349–374.
- (22) Mackay, D.; Shiu, W. Y.; Maijanen, A.; Feenstra, S. J. *Contam. Hydrol.* **1991**, *8*, 23–42.
- (23) Rixey, W. G.; Johnson, P. C.; Deeley, G. M.; Byers, D. L. Dortch, I. J. In *Hydrocarbon Contaminated Soils*, Vol. 1; Calabrese, E. J., Kostecki, P. T., Eds.; Lewis Publishers: Chelsea, MI, 1991; Chapter 28, pp 387–409.
- (24) Malone, D. R.; Kao, C. M.; Borden, R. C. *Water Resour. Res.* **1993**, *29*, 2203–2213.
- (25) Sleep, B. E.; Sykes, J. F. *Water Resour. Res.* **1993**, *29*, 1709–1718.
- (26) Gandhi, P.; Erickson, L. E.; Fan, L. T. *J. Hazard. Mater.* **1995**, *41*, 185–204.
- (27) Lee, K. Y.; Chrysikopoulos, C. V. *Environ. Geol.* **1995**, *26*, 157–165.
- (28) Peters, C. A.; Labieniec, P. A.; Knightes, C. D. *Non-Aqueous Phase Liquids (NAPLs) in Subsurface Environment: Assessment and Remediation*; Proceedings of a Specialty Conference at the ASCE 1996 National Convention; ASCE: New York, 1996; pp 681–692.
- (29) Blackburn, E. A. Modeling the Dissolution and Transport of a Multicomponent NAPL. MSE Dissertation, Princeton University, Princeton, NJ, 1998.
- (30) Peters, C. A.; Luthy, R. G. *Environ. Sci. Technol.* **1993**, *27*, 2831–2843.
- (31) Banerjee, S. *Environ. Sci. Technol.* **1984**, *18*, 587–591.
- (32) Burris, D. R.; MacIntyre, W. G. *Environ. Toxicol. Chem.* **1985**, *4*, 371–377.
- (33) Lane, W. F.; Loehr, R. C. *Environ. Sci. Technol.* **1992**, *26*, 983–990.
- (34) Lee, L. S.; Hagwell, M.; Delfino, J. J.; Rao, P. S. C. *Environ. Sci. Technol.* **1992**, *26*, 2104–2110.
- (35) Peters, C. A.; Mukherji, S.; Weber, W. J., Jr. *Environ. Toxicol. Chem.* **1999**, *18*, 426–429.
- (36) Ripp, J.; Taylor, B.; Mauro, D.; Young, M. *Chemical and Physical Characteristics of Tar Samples from Selected Manufactured Gas Plant (MGP) Sites*; EPRI TR-102184; Electric Power Research Institute: Palo Alto, CA, 1993.
- (37) Mercer, J. W.; Cohen, R. M. *J. Contam. Hydrol.* **1990**, *6*, 107–163.
- (38) LeBlanc, D. R.; Garabedian, S. P.; Hess, K. M.; Gelhar, L. W.; Quadri, R. D.; Stollenwerk, K. G.; Wood, W. W. *Water Resour. Res.* **1991**, *27*, 895–910.
- (39) Imhoff, P. T.; Jaffé, P. R.; Pinder, G. F. *Water Resour. Res.* **1993**, *30*, 307–320.
- (40) *Risk Assessment Guidance for Superfund Volume I: Human Health Evaluation Manual (Part A)*; Office of Emergency and Remedial Response, U.S. Environmental Protection Agency: Washington, DC, 1989; EPA/540/1-89/002.
- (41) Krewski, D.; Thorslund, T.; Withey, J. *Toxicol. Ind. Health* **1989**, *5*, 851–867.
- (42) National Research Council. *Complex Mixtures Methods for In Vivo Toxicity Testing*; National Academy Press: Washington, DC, 1988.
- (43) *Risk Assessment Guidance for Superfund Volume I: Human Health Evaluation Manual Supplemental Guidance 'Standard Default Exposure Factors' Interim Final*; Office of Emergency and Remedial Response, U.S. Environmental Protection Agency: Washington, DC, 1991; PB91-921314.
- (44) *Cleaning Up the Nation's Waste Sites: Markets and Technology Trends 1996 Edition*; Office of Solid Waste and Emergency Response, U.S. Environmental Protection Agency: Washington, DC, 1997; EPA-542-R-96-005.
- (45) Hess, K. M.; Wolf, S. H.; Celia, M. A. *Water Resour. Res.* **1992**, *28*, 2011–2027.
- (46) Roy, S. B.; Dzombak, D. A.; Ali, M. A. *Water Environ. Res.* **1995**, *67*, 4–15.
- (47) Ali, M. A.; Dzombak, D. A.; Roy, S. B. *Water Environ. Res.* **1995**, *67*, 16–24.
- (48) Knightes, C. D.; Peters, C. A. *WEFTEC'96*, Proceedings of Water Environmental Federation 69th Annual Conference Vol. I, Part I: Wastewater Treatment Research; 1996; pp 333–343.
- (49) Judge, C.; Kostecki, P.; Calabrese, E. *Soil Groundwater Cleanup* **1997**, November, 10–34.
- (50) Mackay, D. M.; Cherry, J. A. *Environ. Sci. Technol.* **1989**, *23*, 630–636.
- (51) *1995 CERCLA Priority List of Hazardous Substances That Will Be the Subject of Toxicological Profiles & Support Documents*; U.S. Department of Health and Human Services, Agency for Toxic Substances and Disease Registry (ATSDR): Atlanta, 1996.

Received for review November 20, 1998. Revised manuscript received August 30, 1999. Accepted September 3, 1999.

ES981203E